MRS Communications (2017), 7, 967–973

doi:10.1557/mrc.2017.127

MRS Communications

Research Letter

N-Phenyl naphthalene diimide pendant polymer as a charge storage material with high rate capability and cyclability

Subashani Maniam, School of Chemistry, Monash University, Wellington Rd., Clayton 3800, Victoria, Australia
Kouki Oka and **Hiroyuki Nishide,** Department of Applied Chemistry, Waseda University, Tokyo 169-8555, Japan
Address all correspondence to Subashani Maniam, Hiroyuki Nishide at **subashani.maniam@monash.edu**, **nishide@waseda.jp**

(Received 2 October 2017; accepted 6 November 2017)

Abstract

Pendent-type polymers are attractive materials which allow the flexibility to introduce various redox active moieties that facilitate rapid ion/electron transport and enable charge storage. Here, we demonstrate naphthalene diimide polymers with polynorbornene backbone having *N*-phenyl, PNAn **5** and *N*-(4-nitrophenyl), PNNO **6**. Small changes in the molecular design have led to a significant difference in bulk material and device properties. PNNO **6** maintained 80% of its capacity at 1C after 10 cycles in a Li-ion coin cell. PNAn **5** displayed exceptionally high charge capacity and rate capability with excellent cyclability, maintaining almost its theoretical capacity at various C-rates throughout 500 cycles.

Introduction

Traditionally, the materials used for electrochemical energy storage systems are metal-based inorganic compounds, such as cobalt, iron, tin, and manganese for lithium battery electrodes and vanadium oxides for redox flow batteries.[1] These inorganic materials rely heavily on the oxidation states of the metals for charge storage and the stabilization of the charge by the counter ion. Although some of these metals work well giving reasonable output voltage, they are relatively scarce, heavy and toxic and their production requires expensive high-temperature processing.[2] Organic materials provide an excellent alternative and versatile platform to be developed into new and exciting materials for charge storage systems. Organic materials can easily be derivatized using simple building blocks to tune the electrochemical properties. Thus the same organic material can be developed for a wide variety of different charge storage devices such as lithium, all organic and multivalent ion batteries.[1] Their performance, however, is limited by the tendency to dissolve in organic electrolytes which compromises charge-discharge cycles or cyclability. It is important for the organic material to be solvated by the electrolyte to allow interpenetration of the counter ions in the electrode. There have been various efforts focused on increasing cyclability by introducing rigid aromatic groups,[3,4] insoluble salts,[5] and macromolecular materials.[6–12] Polymers can be designed to be insoluble in electrolyte solution while still retaining the high theoretical capacity (C_{theor}) of small molecules. As a result, polymer-based materials with carbonyl groups have gained popularity, such as anhydrides and quinones which have proven to achieve significant progress.[1,13–15]

Naphthalene diimide (NDI) is the smallest class of aromatic carbonyl compound from the rylene family that displays tremendous chemical, thermal and photochemical stability, thus has been widely used as n-type material in organic electronics.[16] For example, the NDI moieties work as an electron accepting unit leading to an excellent charge separation in star-shaped triphenylamine-NDI molecules for solar cell purposes.[17] NDI also perform electrochemical redox due to its electron deficient aromatic ring which leads to its application as sensors for detection of anions in solution.[18] We have extensively investigated organic redox polymer-based rechargeable devices and have shown that phthalimide and pyromellitic polyimides formed on carbon nanofibers are capable to perform as electrode-active material.[19] NDIs have been incorporated in polymers as part of the backbone to introduce rigidity, increase electron mobility, and thermal stability. However, such polymers lack in solubility and processability.[13] Alternatively, NDIs are applied as pendant side chains with insulating backbone. Qin et al. have demonstrated using NDI as part of the polymer backbone in aqueous-based batteries to have a capacity of 70 mAh/g at 2C with 20% decrease of the initial capacity after 200 cycles.[20] Another study, yet again NDI as part of the polymer backbone in Li-based batteries has revealed a high capacity of 163 mAh/g at 0.2C with 5% decrease in capacity only after 50 cycles.[6] A star-shaped repeat unit was synthesized with NDI and tris(4-aminophenyl)-benzene to give a microporous polymer which was investigated in Li-based batteries to give a capacity of 103 mAh/g at 0.2C, however, this capacity drastically decreased by 66% only after 30 cycles.[21] Recently, we demonstrated that pendant-type polynorbornene

backbone formed from ring-opening metathesis polymerization improves solubility of NDI for processing, by hindering molecular stacking.[7] The imide functionality for these polymers were aliphatic groups, which inherently increases the solubility of NDIs. Consequently, crosslinking of the polynorbornene backbone double bonds were required to prevent dissolution of the polymer in the electrolyte solution. The *N*-methyl NDI polymer maintained only 70% of its capacity at 20C and the cyclability decreased 10% over 100 cycles in Li-ion batteries.

In this work, we report the properties of two pendant-type polynorbornene, with one bearing a simple phenyl group and the other with nitro at the para position. A small alteration in the molecular design shows a significant change in the device performance. The simple phenyl polymer display consistent high-rate discharging/charging capability, relatively high-voltage output with excellent cyclability in Li-ion coin cells, maintaining values almost the theoretical capacity. These polymers do not require photo-crosslinking as they form insoluble polymer layer.

Experimental details

Synthesis of monomers and polymers

N-*(5-Norbornene-2-methyl) naphthalene-1,4,5,8-tetracarboxylic monoanhydride monoimide (**2**)*

Compound **2** was synthesized by modifying method in literature.[22] 1,4,5,8-Naphthalene tetracarboxylic dianhydride **1** (2.80 g, 10.4 mmol) was suspended in water (400 mL). KOH pallets were added while stirring until complete dissolution of the starting material. The pH of the solution was adjusted to 6.4 with 1 M phosphoric acid solution addition. 5-Norbornene-2-methylamine (1.26 g, 10.2 mmol) was added and the pH was adjusted to 6.4 using 1 M phosphoric acid solution. The reaction mixture was heated at reflux for 12 h. The reaction was allowed to cool to room temperature and acidified to pH 1–2 with glacial acetic acid. The precipitation formed was filtered and washed with methanol (50 mL) and *n*-hexane (50 mL) to give **2** as a white powder (*endo*/*exo* = 80/20) (3.50 g, 90%). M.p. 226–227 °C. ^{1}H NMR (DMSO-d_6, 400 MHz) δ 8.55–8.54 (m, 2H, NDI), 8.18–8.16 (m, 2H, NDI), 6.26 (dd, J = 5.6 & 2.8 Hz, 0.8H, *endo*), 6.17 (dd, J = 5.6 & 2.8 Hz, 0.8H, *endo*), 6.04 (dd, J = 5.6 & 2.8 Hz, 0.2H, *exo*), 5.98 (dd, J = 5.6 & 2.8 Hz, 0.2H, *exo*), 4.10–4.06 (m, 0.4H, *exo*), 3.81–3.72 (m, 1.6H, *endo*), 2.82–2.72 (m, 1.6H, *endo*), 2.58–2.49 (m, 0.4H, *exo*), 1.88–1.82 (m, 0.8H, *endo*), 1.55–1.53 (m, 0.2H, *exo*), 1.34–1.23 (m, 2H), 1.20–1.16 (m, 1H), 0.70–0.66 (m, 1H). ^{13}C NMR (DMSO-d_6, 400 MHz) δ 168.6, 163.2, 162.9, 137.2, 137.1, 136.7, 136.3, 133.1, 130.2, 130.1, 129.1, 128.54, 128.45, 125.5, 124.4, 49.0, 44.9, 44.0, 43.9, 43.5, 41.9, 41.2, 37.3, 37.2, 30.2, 21.0. HR-ESI-MS *m*/*z* obsd $[M]^+$ 373.0959, calcd $C_{22}H_{15}NO_5$ $[M]^+$ 373.0950.

N-*(5-Norbornene-2-methyl)*-N′-*(phenyl)-naphthalene-1,4,5,8-tetracarboxyl diimide (**3**)*

A mixture of compound **2** (200 mg, 0.54 mmol) and aniline (74.8 mg, 0.80 mmol) in acetic acid (30 mL) was heated at 130 °C for 8 h. Then, the reaction was cooled to room temperature which resulted in the formation of crystalline solid precipitates. The solid was collected by filtration. The crude product was purified by recrystallization from DCM/methanol to obtain the final products **3** as white solid (*endo*/*exo* = 80/20) (200 mg, 83%). M.p. > 290 °C. ^{1}H NMR ($CDCl_3$, 400 MHz) δ 8.85–8.78 (m, 4H, NDI), 7.61–7.50 (m, 4H, phenyl), 7.36–7.31 (m, 1H, phenyl), 6.32 (dd, J = 5.6 & 2.8 Hz, 0.8H, *endo*), 6.27 (dd, J = 5.6 & 2.8 Hz, 0.8H, *endo*), 6.08 (dd, J = 5.6 & 2.8 Hz, 0.2H, *exo*), 6.02 (dd, J = 5.6 & 2.8 Hz, 0.2H, *exo*), 4.31–4.28 (m, 0.4H, *exo*), 4.02–3.98 (m, 1.6H, *endo*), 2.90–2.78 (m, 2H), 2.66–2.58 (m, 1H), 2.05–1.93 (m, 1H), 1.94–1.67 (m, 1H), 1.46–1.23 (m, 1H), 0.84–0.79 (m, 1H). ^{13}C NMR ($CDCl_3$, 400 MHz) δ 163.3, 163.2, 163.1, 138.0, 137.3, 134.8, 133.1, 131.6, 131.5, 131.3, 131.2, 129.7, 129.3, 128.6, 127.22, 127.17, 127.1, 127.0, 126.9, 126.8, 49.7, 44.8, 42.6, 38.1, 30.8. HR-ESI-MS *m*/*z* obsd $[M]^+$ 448.1419, calcd $C_{28}H_{20}N_2O_4$ $[M]^+$ 448.1423.

N-*(5-Norbornene-2-methyl)*-N′-*(4′-nitrobenzene)-naphthalene-1,4,5,8-tetracarboxyl diimide (**4**)*

A mixture of compound **2** (200 mg, 0.54 mmol) and 4-nitroaniline (111 mg, 0.80 mmol) in acetic acid (30 mL) was heated at 130 °C for 8 h. Then, the reaction was cooled to room temperature which resulted in the formation of crystalline solid precipitates. The solid was collected by filtration. The crude product was purified by recrystallization from DCM/methanol to obtain the final products as a pale yellow solid (*endo*/*exo* = 80/20) (214 mg, 81%). M.p. 143 °C. ^{1}H NMR ($CDCl_3$, 400 MHz) δ 8.84–8.80 (m, 4H, NDI), 8.45–8.43 (m, 2H, phenyl), 7.57–7.54 (m, 2H, phenyl), 6.32 (dd, J = 5.6 & 2.8 Hz, 0.8H, *endo*), 6.24 (dd, J = 5.6 & 2.8 Hz, 0.8H, *endo*), 6.07 (dd, J = 5.6 & 2.8 Hz, 0.2H, *exo*), 6.00 (dd, J = 5.6 & 2.8 Hz, 0.2H, *exo*), 4.31–4.27 (m, 0.4H, *exo*), 4.00–3.97 (m, 1.6H, *endo*), 2.90–2.62 (m, 2H), 2.61–2.58 (m, 1H), 2.09–1.93 (m, 1H), 1.94–1.67 (m, 1H), 1.48–1.21 (m, 1H), 0.84–0.77 (m, 1H). ^{13}C NMR ($CDCl_3$, 400 MHz) δ 162.9, 162.8, 162.5, 159.0, 148.2, 140.4, 138.04, 138.02, 137.3, 133.3, 131.8, 131.5, 130.2, 129.0, 128.1, 127.6, 127.0, 126.2, 124.9, 122.9, 49.7, 45.0, 44.9, 44.8, 42.6, 38.1, 30.8. HR-ESI-MS *m*/*z* obsd $[M]^+$ 493.1273, calcd $C_{28}H_{19}N_3O_6$ $[M]^+$ 493.1274.

*Polymer PNAn **5***

A solution of Grubbs 2nd generation (1.76 mg, 2.82 μmol) in chloroform (0.4 mL) was added to a solution of **3** (100 mg, 0.22 mmol) in chloroform (4 mL). The mixture was stirred for 12 h at 60 °C under nitrogen atmosphere. Then, the resulting polymerization reaction mixture was poured into hexane, and the precipitated polymer was purified by reprecipitation from chloroform into methanol. This purification process was repeated once more to give polymer **PNAn** as white solid (60 mg) Tg = 354.4 °C, Mn = 7330, M_w/M_n = 2.0; ^{1}H NMR ($CDCl_3$, 400 MHz) δ 8.78–8.35 (br m, 4H, NDI), 7.65–7.40 (br m, 4H, phenyl), 7.25–7.10 (br m, 1H, phenyl), 5.80–5.15 (br m, 2H), 4.40–3.80 (br m, 2H), 3.25–3.2.30 (br m, 3H), 2.20–1.15 (br m, 4H).

https://doi.org/10.1557/mrc.2017.127

*Polymer PNNO **6***

A solution of Grubbs 2nd generation (1.76 mg, 2.82 μmol) in chloroform (0.4 mL) was added to a solution of **4** (110 mg, 0.22 mmol) in chloroform (4 mL). The mixture was stirred for 12 h at 60 °C under nitrogen atmosphere. Then, the resulting precipitate was filtered and washed with chloroform (200 mL) to give polymer **PNNO** as white solid (82 mg). This insoluble polymer **6** was only characterized by thermal analysis. Tg = 343.6 °C.

Electrochemical measurements

The electrochemical measurements were performed under nitrogen using tetraethylammonium perchlorate (TEAP) in acetonitrile as the electrolyte for the all organic half-cell. A potentiostat/galvanostat system (BAS Inc. ALS660D) was used for the cyclic voltammetry, chronopotentiometry, and chronoamperometry experiments. The working potential was measured against Ag/AgCl reference electrode and, platinum disk and coiled platinum wire were used as the working and counter electrode, respectively. Cyclic voltammograms of the polymer electrodes for the Li-ion half-cell were measured in 1 M lithium perchlorate ($LiClO_4$) electrolyte in γ-butyrolactone (GBL) solution.

Coin cell fabrication

Coin cells were fabricated by sandwiching the electrolyte layer of 1 M $LiClO_4$ in GBL solution with a lithium metal as the anode and the polymer as at the cathode, using a separator film (UP3085 from Ube Industries Co.) in a glove box under a dry argon atmosphere. The cyclability performance of the fabricated cell was tested by repeated discharge-charge galvanostatic cycles with the cut-off potentials 0–4.8 V versus Li/Li^+.

Discussion

A convergent synthetic strategy was used to access monomers **3** and **4** (Scheme 1). 1,4,5,8-Naphthalenetetracarboxylic dianhydride, NDA **1** was subjected to a mono-imidation reaction to give **2**, which is then treated with the corresponding anilines to obtain the dissymmetric NDI monomers **3** and **4**. Firstly, the redox properties of both of the monomers were characterized using cyclic voltammetry. Two reversible reduction potentials were recorded at $E_{1/2}$ at −0.90 and −1.30 V (versus Ag/AgCl) for **3** and $E_{1/2}$ at −0.81 and −1.23 V (versus Ag/AgCl) for **4** (see Fig. S8, ESI), consistently displaying two electron-redox mechanism as seen for previously reported NDI compounds.[23] The effect of the nitro substituent can be seen by the shift of the redox properties towards more positive potentials versus Ag/AgCl. With these promising indications, monomers **3** and **4** were put through to the next synthetic step.

PNAn **5** and PNNO **6** were polymerized from **3** and **4**, respectively via ring-opening metathesis reaction to give access to polymers with high molecular weight. PNAn was sparingly soluble in chlorinated solvents such as dichloromethane and chloroform, however, PNNO was rather insoluble in these solvents but displayed some solubility in DMSO and DMF. The drop casting solutions of **5** and **6** on the glass for UV-Vis analysis gave homogenous polymer layers. Both spectra show the characteristic structured bands in the near-UV at 350 and 370 nm, assigned to the π–π^* transition of the NDI [Figs. 1(a) and 1(b)]. These spectral features are consistent with previously reported NDIs.[24] PNAn **5** shows NDI aggregation in the solid state as shown by the tailing above 400 nm however this is not observed in the monomer, **3**. For **4**, NDI aggregation is seen in the monomer and this phenomenon is intensified in the polymer PNNO **6**.

Carbon composite electrodes consisting of **5** and **6** combined with vapor-grown carbon fiber (VGCF) as the conductive additives and poly(vinylidene fluoride) (PVDF) as the binder were used to evaluate the electrochemical properties of the polymers. Firstly, 0.1 M tetrabutylammonium perchlorate (TBAP)/acetonitrile solution was used as the electrolyte, however, upon reduction, the polymers started to dissolve. Even at 1 M concentration of this electrolyte, polymer dissolution was

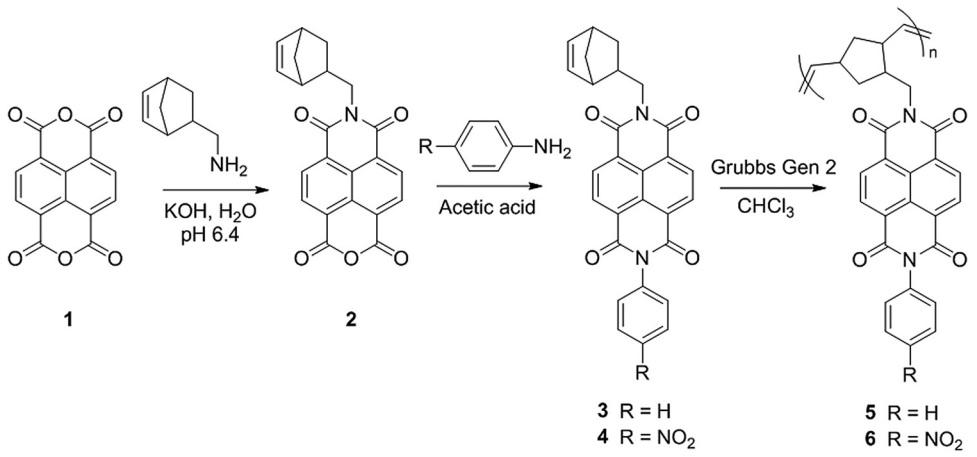

Scheme 1. Synthesis of PNAn **5** and PNNO **6**.

https://doi.org/10.1557/mrc.2017.127

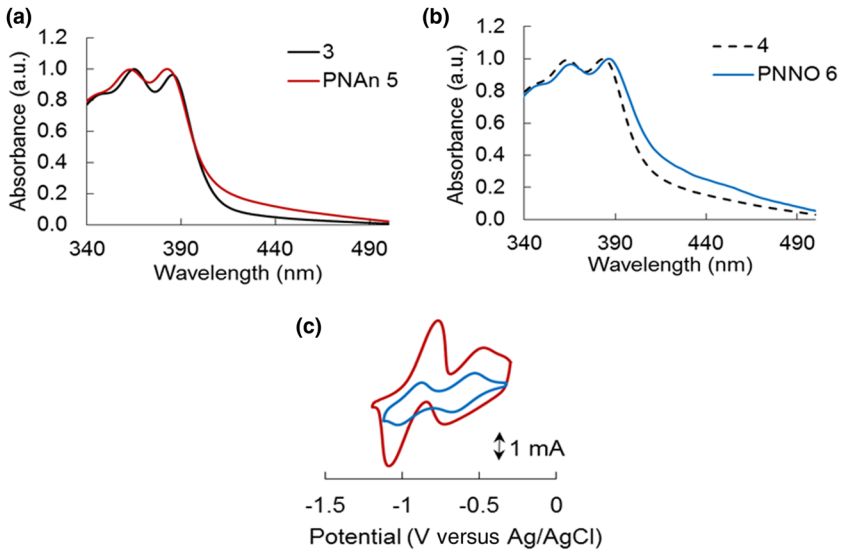

Figure 1. UV-Vis spectra of the polymers (a) **5** and (b) **6** and their corresponding monomers on a glass substrate. (c) Cyclic voltammograms of **5** (maroon) and **6** (blue) in 1 M TEAP/acetonitrile electrolyte at a scan rate of 10 mV/s.

observed however slower decrease in current was recorded over several scans (see Fig. S9, ESI). At higher electrolyte concentration presumably ionic pairing occurs much faster, resulting in slower polymer dissolution. When the cation is changed to the tetraethyl, a smaller cation which allows easier ion migration from and in the polymer matrix, both polymers did not show any dissolution. Thus, in 1 M tetraethylammonium perchlorate (TEAP)/acetonitrile solution the cyclic voltamograms were recorded for polymers **5** and **6**. Both polymers displayed two reversible redox potentials as shown in Fig. 1(c) without current decrease during the repeated scans (see Fig. S10, ESI). Polymer **5** had half-wave potentials, $E_{1/2}$ at −0.63 and −0.92 V (versus Ag/AgCl) and polymer **6** gave $E_{1/2}$ at −0.56 and −0.93 V (versus Ag/AgCl). The more positive potentials relative to that of the monomers indicate strong stabilization of the NDI anion by the counter ion in the polymer.[25] It should be noted that for polymer **5**, equal peak currents for the first and second redox potentials were observed, suggesting that each one is a similar process involving a single electron.

Cyclic voltammograms of polymers **5** and **6** were also recorded in 1 M $LiClO_4$/γ-butyrolactone (GBL), which is one of the most common conducting salt used in Li-ion batteries[13] (see Fig. S10, ESI). Consistently, both polymers displayed two redox potentials, with $E_{1/2}$ at −0.61 and −0.79 for **5**, and $E_{1/2}$ at −0.49 and −0.71 for polymer **6** without current decrease during the scans displaying the stability and insolubility of these polymers which are essential for device performance. The potentials were shifted to more positive potentials compared with in TEAP due to higher ionic interactions.[25] The redox process has previously been suggested to occur via an enolate anion formation as shown in Scheme 2. The morphology of the carbon composite electrodes was evaluated by field emission-scanning electron microscopy (FE-SEM) (Fig. 2 and see Fig. S15, ESI).

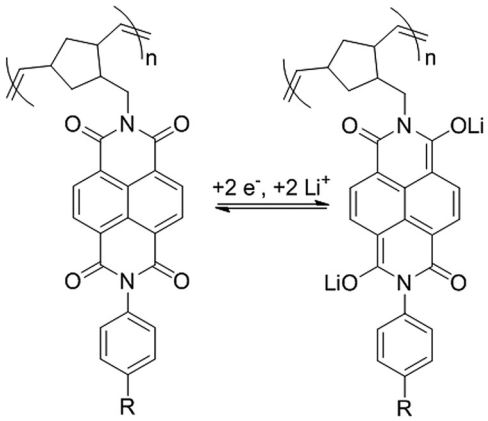

Scheme 2. Redox reactions of the NDI moieties on norbornene polymer.

Spherical particles of the polymer and carbon fibers were uniformly distributed in the composite matrix, allowing ease of counter ion mobility from and in the polymer. There were comparatively little changes in morphology and no collapses or structural damages were observed after 100 cycles of cyclic voltammetry for both polymers. This further supports the durability and robustness of these polymers for a battery application.

The charge storage capability of both **5** and **6** was tested using the coin-cell construct with the polymers as the cathode, lithium foil as the anode, microporous membrane as the separator (UP3085), and 1 M $LiClO_4$/GBL as the electrolyte. Polymers **5** and **6** have a high theoretical capacity of 120 and 109 mAh/g, respectively. Thus, we anticipate that they will behave efficiently as cathode active material. Cyclic voltammograms of polymers **5**

https://doi.org/10.1557/mrc.2017.127

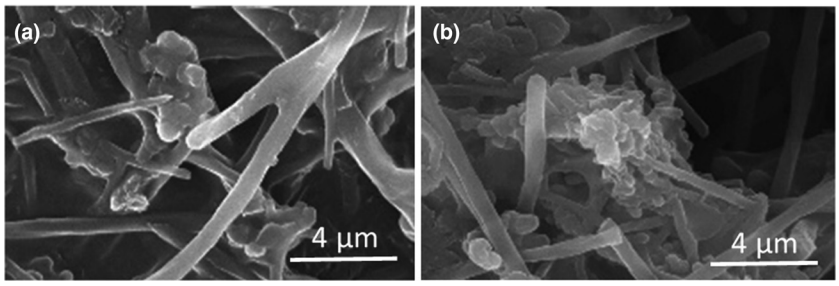

Figure 2. FE-SEM images of the carbon composite redox materials (a) **5** and (b) **6**.

and **6** showed pronounce difference in their profile as compared with those obtained in solution (inset Fig. 3). Polymer **5** and **6** exhibited one reversible redox potentials $E_{1/2}$ at 2.5 versus Li/Li^+. The relatively large shift in the position of the potentials and broadening, suggests kinetic limitations associated with electron and Li^+ ion transport in the bulk solid material.

Thus, we decided to estimate the diffusion coefficient, D for **5** and **6** from chronoamperograms of the polymer layers using the Cottrell equation in the potential range 0 to −1.4 V versus Ag/AgCl (see Fig. S12, ESI). The D values for polymers **5** and **6** were of the order of 10^{-10} cm^2/s^{-1}, comparable with those recorded previously for acrylamide- and norbornene-based polymers, both in aqueous and organic electrolytes for rechargeable charge storage devices.[26] Polymer **5** has a slightly higher D as a result of the phenyl groups allowing π–π stacking between the adjacent polymer chain to gain better electron and charge transport process in addition to the stacking contributed by the NDI core. In polymer **6**, the bulky nitro group would probably hinder this phenyl stacking ability.[27,28]

Galvanostatic cyclic experiments were conducted by recording cell potentials versus time it takes between two potentials upon applying a constant predetermined current. The 1C rate is the current applied which takes 1 h to charge or discharge the entire theoretical capacity. PNAn **5** and PNNO **6** were evaluated at 1C, 5C, 10C, and 20C. Upon application of voltage, a plateau was observed at their $E_{1/2}$ and the potential remained at this value until a new redox event or the material reaches the upper limit of its capacity which was set at 4.8 V. In agreement with the cyclic voltammetry (inset Fig. 3), **5** and **6** displayed only one plateau, despite the two-electron redox mechanism.

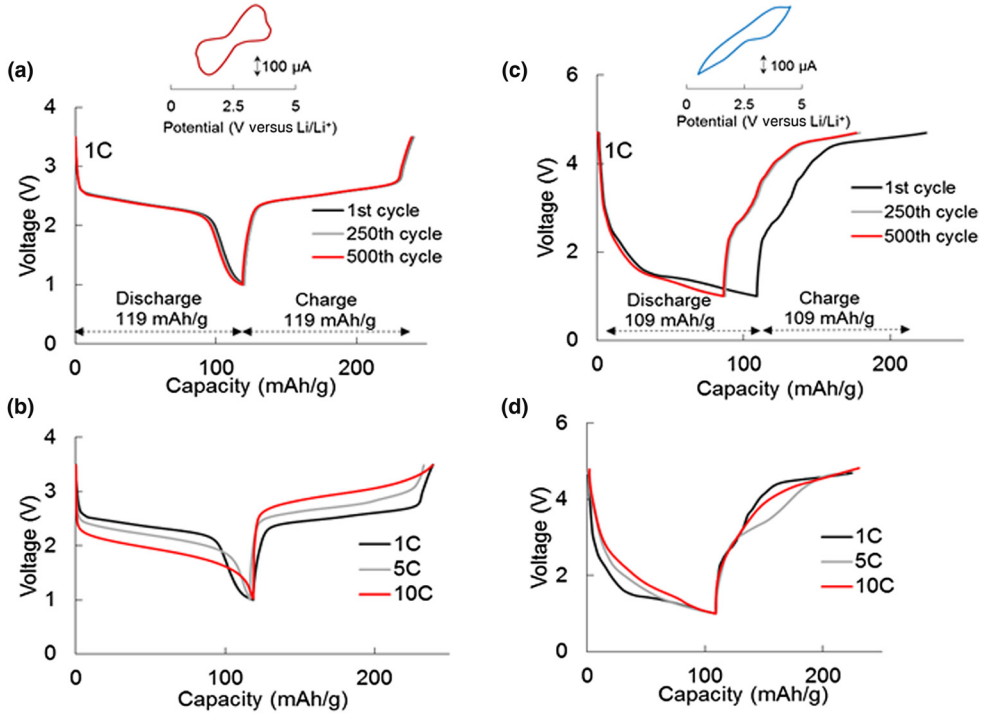

Figure 3. Discharging and charging curves of the coin-cells fabricated with polymer **5** (a) and (b), and polymer **6** (c) and (d).

https://doi.org/10.1557/mrc.2017.127

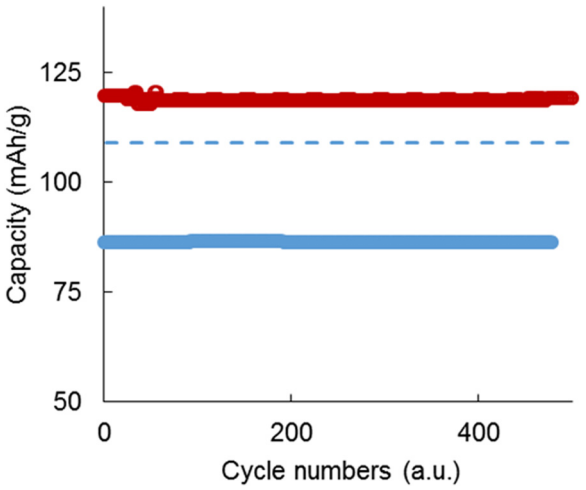

Figure 4. Cycle performance of coin cells fabricated with polymers **5** (maroon) and **6** (blue) cathode. Corresponding theoretical capacities are indicated by the dashed lines.

This is possibly due to the fast kinetics giving cyclic voltammogram curves present serious peak overlap and the discharge/charge curves present only one plateau.[7,25] The coulombic efficiencies (the ratio of discharging versus charging capacity) were over 98% for both polymers at lower C rates. The cyclic voltammograms of coin cells of **5** showed hardly any change in the current over 500 cycles, however, for polymer **6**, a slight decrease in current was observed (see Fig. S11, ESI). Interestingly, **5** maintained similar discharging and charging capacity of 119 mAh/g at 1C over these long cycles, suggesting that almost all of the NDI moieties contribute consistently to charge storage [Fig. 3(a)]. Polymer **5** also displayed good discharging capacity retention at higher C rates even after 500 cycles [Fig. 3(b)] and displayed excellent cyclability properties at all tested C-rates (see Fig. S13, ESI). At 1C, after 500 cycles, polymer **6** maintained 87 mAh/g discharging capacity [Fig. 3(c)]. At higher C rates, polymer **6** continued to display discharging capacity retention above 80% with 5C and 10C being 88 and 93 mAh/g, respectively (see Fig. S14, ESI) after 500 cycles. At all C rates for polymer **6** [Fig. 3(d)], lack of voltage plateaus in the charge and discharge curves were observed which indicate minimal redox activity such as lack of electrolyte solvent affinity and counter ion mobility. This phenomenon is consistent with the lower diffusion coefficient recorded for polymer **6** compared with **5**.

Figure 4 shows the cyclability performance of polymers **5** and **6** at 1C. Throughout these cycles, polymer **5** showed excellent cyclability by maintained values almost the theoretical capacity. Polymer **6**, however, showed capacity decay during the initial cycles, then retained 80% of the initial capacity. Although many factors can account for this observation such as texture, morphology and crystal lattice,[13] the capacity loss of polymer **6** is suggested to be slow diffusion and poor polymer swelling that hinder Li-ions and electron moving throughout the polymer material.

Conclusions

In conclusion, we have shown the potential of two norbornene pendant-type NDI polymers with phenyl, PNAn **5** and *p*-nitrophenyl PNNO **6** as rechargeable charge storage devices. While polymer **6** showed insolubility in most organic solvents which is a good indication for preventing dissolution in organic electrolytes, it only maintained 80% of its capacity at 1C after long cycles. Polymer **5** had high charge capacity and rate capability with excellent cyclability. This new promising, simple-structured redox-active polymer **5** is shown to have controllable discharge/charge potentials and is expected to be usable in other types of rechargeable batteries. These results illustrate the importance of molecular structure and bulk material properties in electrochemical behavior and charge storage.

Supplementary material

The supplementary material for this article can be found at https://doi.org/10.1557/mrc.2017.127

Acknowledgments

Financial support from the Victorian Government, Australia through the Victorian Fellowship under Victorian Endowment for Science Knowledge and Innovation (VESKI) is greatly acknowledged. We also acknowledge the partial support from the Research Institute for Science and Engineering Waseda University. We thank Prof. Kenichi Oyaizu and Dr. Takeo Suga for their invaluable comments on this communication.

References

1. T.B. Schon, B.T. McAllister, P.-F. Li, and D.S. Seferos: The rise of organic electrode materials for energy storage. *Chem. Soc. Rev.* **45**, 6345 (2016).
2. P. Poizot and F. Dolhem: Clean energy new deal for a sustainable world: from non-CO_2 generating energy sources to greener electrochemical storage devices. *Energy Environ. Sci.* **4**, 2003 (2011).
3. Y. Liang, Z. Tao, and J. Chen: Organic electrode materials for rechargeable lithium batteries. *Adv. Energy Mater.* **2**, 742 (2012).
4. H. Nishide and K. Oyaizu: Toward flexible batteries. *Science* **319**, 737 (2008).
5. H. Chen, M. Armand, G. Demailly, F. Dolhem, P. Poizot, and J.-M. Tarascon: From biomass to a renewable $Li_xC_6O_6$ organic electrode for sustainable Li-ion batteries. *ChemSusChem* **1**, 348 (2008).
6. Z. Song, H. Zhan, and Y. Zhou: Polyimides: promising energy-storage materials. *Angew. Chem. Int. Ed. Engl.* **49**, 8444 (2010).
7. Y. Sasada, S.J. Langford, K. Oyaizu, and H. Nishide: Poly(norbornyl-NDIs) as a potential cathode-active material in rechargeable charge storage devices. *RSC Adv.* **6**, 42911 (2016).
8. W. Choi, D. Harada, K. Oyaizu, and H. Nishide: Aqueous electrochemistry of poly(vinylanthraquinone) for anode-active materials in high-density and rechargeable polymer/air batteries. *J. Am. Chem. Soc.* **133**, 19839 (2011).
9. T. Kawai, K. Oyaizu, and H. Nishide: High-density and robust charge storage with poly(anthraquinone-substituted norbornene) for organic electrode-active materials in polymer-air secondary batteries. *Macromolecules* **48**, 2429 (2015).
10. T. Suzuki, T. Sato, J. Zhang, M. Kanao, M. Higuchi, and H. Maki: Electrochemically switchable photoluminescence of an anionic dye in a

cationic metallo-supramolecular polymer. *J. Mater. Chem. C* **4**, 1594 (2016).
11. F. Li, D.N. Gore, S. Wang, and J.L. Lutkenhaus: Unusual internal electron transfer in conjugated radical polymers. *Angew. Chem., Int. Ed.* **56**, 9856 (2017).
12. M.A. Morris, H. An, J.L. Lutkenhaus, and T.H. Epps: Harnessing the power of plastics: nanostructured polymer systems in lithium-ion batteries. *ACS Energy Lett.* **2**, 1919 (2017).
13. S. Muench, A. Wild, C. Friebe, B. Haeupler, T. Janoschka, and U.S. Schubert: Polymer-based organic batteries. *Chem. Rev.* **116**, 9438 (2016).
14. Y. Iizuka, M. Tanaka, and H. Kawakami: Preparation and proton conductivity of phosphoric acid-doped blend membranes composed of sulfonated block copolyimides and polybenzimidazole. *Polym. Int.* **62**, 703 (2013).
15. T. Tamura and H. Kawakami: Aligned electrospun nanofiber composite membranes for fuel cell electrolytes. *Nano Lett.* **10**, 1324 (2010).
16. X. Zhan, A. Facchetti, S. Barlow, T.J. Marks, M.A. Ratner, M.R. Wasielewski, and S.R. Marder: Rylene and related diimides for organic electronics. *Adv. Mater.* **23**, 268 (2011).
17. K. Rundel, S. Maniam, K. Deshmukh, E. Gann, S.K.K. Prasad, J.M. Hodgkiss, S.J. Langford, and C.R. McNeill: Naphthalene diimide-based small molecule acceptors for organic solar cells. *J. Mater. Chem. A* **5**, 12266 (2017).
18. N.A. Young, S.C. Drew, S. Maniam, and S.J. Langford: Systematically studying the effect of fluoride on the properties of cyclophanes bearing naphthalene diimide and dialkoxyaryl groups. *Chem. – Asian J.* **12**, 1668 (2017).
19. K. Oyaizu, A. Hatemata, W. Choi, and H. Nishide: Redox-active polyimide/carbon nanocomposite electrodes for reversible charge storage at negative potentials: expanding the functional horizon of polyimides. *J. Mater. Chem.* **20**, 5404 (2010).
20. H. Qin, Z.P. Song, H. Zhan, and Y.H. Zhou: Aqueous rechargeable alkali-ion batteries with polyimide anode. *J. Power Sources* **249**, 367 (2014).
21. D. Tian, H.-Z. Zhang, D.-S. Zhang, Z. Chang, J. Han, X.-P. Gao, and X.-H. Bu: Li-ion storage and gas adsorption properties of porous polyimides. *RSC Adv.* **4**, 7506 (2014).
22. S. Ulrich, A. Petitjean, and J.-M. Lehn: Metallo-controlled dynamic molecular tweezers: design, synthesis, and self-assembly by metal-ion coordination. *Eur. J. Inorg. Chem.* **2010**, 1913 (2010).
23. S. Maniam, S. Sandanayake, E.I. Izgorodina, and S.J. Langford: Unusual products from oxidation of naphthalene diimides. *Asian J. Org. Chem.* **5**, 490 (2016).
24. S.V. Bhosale, C.H. Jani, and S.J. Langford: Chemistry of naphthalene diimides. *Chem. Soc. Rev.* **37**, 331 (2008).
25. C.R. De Blase, K. Hernandez-Burgos, J.M. Rotter, D.J. Fortman, D.d. S. Abreu, R.A. Timm, I.C.N. Diogenes, L.T. Kubota, H.D. Abruna, and W.R. Dichtel: Cation-dependent stabilization of electrogenerated naphthalene diimide dianions in porous polymer thin films and their application to electrical energy storage. *Angew. Chem., Int. Ed.* **54**, 13225 (2015).
26. N. Sano, W. Tomita, S. Hara, C.-M. Min, J.-S. Lee, K. Oyaizu, and H. Nishide: Polyviologen hydrogel with high-rate capability for anodes toward an aqueous electrolyte-type and organic-based rechargeable device. *ACS Appl. Mater. Interfaces* **5**, 1355 (2013).
27. F. Cozzi and J.S. Siegel: Interaction between stacked aryl groups in 1,8-diarylnaphthalenes: dominance of polar/π over charge-transfer effects. *Pure Appl. Chem.* **67**, 683 (1995).
28. C. Glidewell, J.N. Low, J.M.S. Skakle, and J.L. Wardell: 4-Nitrophenyl phenyl ether: sheets built from C-H···O and C-H···pi(Arene) hydrogen bonds. *Acta Crystallogr. C* **61**, 185 (2005).

https://doi.org/10.1557/mrc.2017.127